

WELDABILITY AND MECHANICAL PROPERTIES OF DISSIMILAR AL-MGSI TO PURE ALUMINIUM AND AL-MG USING FRICTION STIR WELDING PROCESS

Nor Fazilah Mohd Selamat^{a*}, Amir Hossein Baghdadi^a, Zainuddin Sajuri^a, Amir Hossein Kokabi^b

^aDepartment of Mechanical & Materials Engineering, Faculty of Engineering and Built Environment, 43600 UKM Bangi Selangor Darul Ehsan, Malaysia

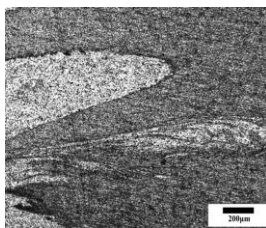
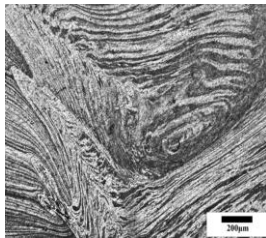
^bDepartment of Materials Science and Engineering, Sharif University of Technology, Tehran Iran

Article history

Received
17 November 2017
Received in revised form
28 August 2018
Accepted
13 September 2018
Published online
15 December 2018

*Corresponding author
zsajuri@ukm.edu.my

Graphical abstract



Abstract

Friction stir welding (FSW) is used to join different lightweight materials, especially aluminium alloys. Dissimilar joints of aluminium alloys have an issue to be weld using the conventional fusion welding. In the present work, two types of dissimilar joints of aluminium alloys were welded as dissimilar butt joints using the FSW method. 5mm thick base metals, consist of AA1100, AA5083 and AA6061, were butt welded to dissimilar joints of AA6061-AA1100 and AA6061-AA5083. Similar welding parameter was used for both of the joints, in which 100 mm/min and 1000 rpm for transverse and rotation speed, respectively. Joints were successful with defect-free internally and externally. However, different flow patterns were observed in the stirred zone due to the different materials flow during the FSW process. The ultimate tensile strength of AA6061-AA1100 and AA6061-AA5083 are 93MPa and 113MPa. Thereby, the joint efficiency of AA6061-AA1100 and AA6061-AA5083 were 80% and 97% compared to AA6061 base metal, respectively.

Keywords: Friction stir welding (FSW), dissimilar joint, nugget zone, mechanical properties, aluminium alloys

Abstrak

Kimpalan geser kacau (FSW) digunakan untuk mengimpal bahan ringan, terutamanya aloi aluminium. Sambungan tak serupa aloi aluminium mempunyai masalah untuk disambung menggunakan kimpalan pelakuran konvensional. Dalam kajian ini, dua jenis sambungan tak serupa telah dikimpal temu menggunakan kaedah FSW. Logam asas berketebalan 5mm yang terdiri daripada aloi aluminium grad AA1100, AA5083 dan AA6061 telah dikimpal menjadi sambungan tak serupa AA6061-AA1100 dan AA6061-AA5083. Parameter kimpalan yang sama telah digunakan bagi kedua sambungan iaitu 100mm/min untuk laju melintang dan 1000rpm bagi laju putar. Sambungan telah berjaya disambung tanpa sebarang kecacatan dalaman dan luaran. Walaubagaimanapun, bentuk aliran bahan pada kawasan terkacau berbeza bagi kedua-dua jenis sambungan disebabkan oleh keberaliran bahan yang berbeza. Kekuatan tegang maksima AA6061-AA1100 dan AA6061-AA5083 masing-masing 93MPa dan 113MPa. Oleh itu, kecekapan sambungan AA6061-AA1100 dan AA6061-AA5083 masing-masing 80% dan 97% apabila dibandingkan dengan logam asas AA6061.

Kata kunci: Kimpal geser kacau, sambungan tak serupa, zon nugget, sifat mekanikal, aloi aluminium

© 2018 Penerbit UTM Press. All rights reserved

1.0 INTRODUCTION

Friction stir welding (FSW) which was invented in 1991 by The Welding Institute is also known as solid state welding [1]. This welding process can overcome the difficulties of producing a sound welding of aluminium alloys by the conventional fusion welding. In essence, the FSW works when the tool pin is plugged in between two base metals [1]. The base metal that located at the side parallel to the welding direction called as the advancing side, and the metal on the other side is known as retreating side. Relative motion in transverse and rotation of the pin with the metals will generate frictional heat that softens the materials under the pin shoulder. Joining of FSW is performed when the materials experience the plastic flow and mix of two metals occur without melting the metal[2].

During the FSW process, the pin has an important role to generate heat by the friction force, while the pin shoulder will confine the materials heated from the movement of the pin [3]. In common, the welding zone consists of different regions, namely thermal-mechanically affected zone (TMAZ), heat affected zone (HAZ) and nugget zone (NZ). Those regions experience a variance of plastic deformations. For example, NZ is fully recrystallized due to a large volume of materials flow due to pin rotation and resulted in TMAZ near to NZ which is mechanically deformed and influenced by heat exerted to the zone. Hence, the HAZ at the outer zone has undergone the thermal cycles without any deformation of microstructures and mechanical properties.

The FSW process leads to the easiness of lightweight metal joining and it is also preferable to weld dissimilar materials since the conventional methods like fusion welding have limitation on dissimilar materials joining. The FSW process is also clean from eliminated waste which leads to an environmentally green process and saves the energy required [3]. Thus, the FSW process is expected to, in the future, to be ubiquitous in industries utilizing lightweight materials. However, there are many factors that dictate the effectiveness of the FSW process vis-à-vis dissimilar materials welding. Commercial aluminium alloys such as AA1100 and AA5083 were known as non-heat treatable and AA6061 as heat-treatable aluminium alloys. These aluminium alloys highly demanded in various industries as structures either single or welded parts. However, the non-heat-treatable or heat-treatable aluminium alloys presented different welding behaviour. The weldability of AA6082 is higher compared to the AA5083 especially in high welding rate, but the effectiveness of joining still depends on the tool dimension and welding parameter [4].

Previous researcher found that the range of welding parameter of the similar joint AA1050 was narrow compared to the similar joint of AA6061 and

the effectiveness of tensile strength was 79% and 77% for AA1050 and AA6061, respectively [5]. The other researcher stated that the dissimilar joints of AA1100 and A441 steel were successfully welded defect free and had good welding surface with rotation speed of 710rpm [6]. In FSW, the welding parameters and the position of advancing side materials gave the benefits of forming sound joints for dissimilar materials. For instant, the threaded cylindrical pin form a defect free joint compared to a straight cylindrical and tapered cylindrical pin with the rotation speed of 1100rpm and transverse speed of 22mm/min [7]. These previous findings showed proved that the dissimilar joints using FSW will have a vast potential to be employed in industries.

Recently, FSW of AA5xxx to AA6xxx has gained numerous interests among researchers due to its high application in the automotive and aviation industries [8]. The AA5083 and AA6061 are relative to high strength to lightweight aluminium alloys, good in corrosion resistant and toughness. These series are widely engaged in the automotive, aircraft and marine industries [9]. AA1100 has outstanding features in corrosion resistant, workability and electrical conductivity [10].

In this research work, the commercial aluminium alloys AA1100, AA5083 and AA6061 were chosen for the FSW process. These aluminium grades have been chosen since it commonly used in the industries. The dissimilar joints of different aluminium grades might give different results in terms of mechanical properties. The aims of this work were to investigate the mechanical properties between two types of dissimilar joints and differentiate the microstructure evolution and mechanical properties of the joints.

2.0 METHODOLOGY

Pure aluminium, Al-Mg and Al-Mg-Si known with grade AA1100, AA5083 and AA6061 were used in this work. These types of aluminium alloys are known as heat-treatable and non-heat-treatable. The chemical compositions and mechanical properties of the alloys are shown in Table 1 and Table 2, respectively.

Table 1 Chemical compositions of base metal (in Wt%)

Gred	Si	Fe	Mn	Mg	Zn	Ti	Al
AA1100	-	0.05	-	0.12	-	0.06	Bal
AA5083	0.25	0.45	1.00	4.46	0.03	0.05	Bal
AA6061	0.52	0.70	0.15	0.88	0.16	0.14	Bal

Table 2 Mechanical properties of base metal

Gred	σ_y (MPa)	σ_{UTS} (MPa)	El.%	Hv _{0.1}
AA1100	71	121	24	45
AA5083	191	328	22	90
AA6061	68	116	29	46

Welding plates with the dimension of 150mm x 100mm x 5mm were fixed and clamped for welding on the table backing plate at FSW machine as shown in Figure 2. Butts joint welding of two dissimilar materials was made which were consisting of AA6061-AA5083 and AA6061-AA1100, correspondingly called as AW65 and AW61. The advancing and retreating sides were determined due to the efficiency of the joint. In this work, the advancing side was the AA5083 for AW65 and the AA6061 for AW61. The welding parameters were the same for both joints. Transverse speed and rotational speed were fixed at 100mm/min and 1000rpm, respectively [11]. The FSW pin tool was made of H13 steel and the tool shoulder's diameter was 20mm. The pin geometry used was simple and threaded with the pin length of 4.7mm and diameter of 5mm; else, the set inclined angle for all samples was 3°.

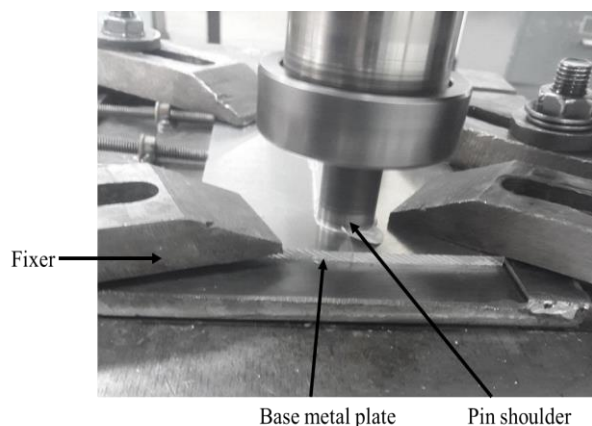


Figure 1 Sample configuration on the fixture table of FSW machine

Metallographic test was acquired by cutting, grinding and polishing the cross section of welding joints. The Weck reagent and Barker's anodizing method were used to observe the microstructure. Barker's anodizing method need 1A and 20V with 90s holding time. The microstructures of welded samples were acquired by optical microscope. Whereas, the fracture surface of samples were observed by scanning electron microscope SEM using 1.0K magnification (Supra 55-Zeiss, German).

Tensile test was conducted using a Zwick universal testing machine (Zwick, German) with 100kN load capacity. The work conducted using procedure of ASTM E8. The dimensions of the tensile sample had the gauge length of 40mm, width of 6mm and 4mm thickness of samples; whereas the cutting samples were perpendicular to the FSW direction. The top and bottom surfaces of the samples were milled off 0.5mm each to eliminate the stress concentration induced by welding flash [12].

Vickers micro-hardness has been taken at the middle along the cross section the weldment. This work was obtained by Vickers micro-hardness (Zwick, German) with the load of 100g and dwell time at 15s.

The distance is 1mm between each indentation, from base metal at advancing side to retreating side.

3.0 RESULTS AND DISCUSSION

3.1 Microstructure of Base Metal

The microstructure of a base metal is shown in Figure 2. The microstructures shows the different size of grain size, as it is related to the mechanical strength of the alloys itself. The grain size of AA1100, AA5083 and AA6061 are 32 μ m, 21 μ m and 26 μ m, respectively. The fine precipitate on the surface of AA5083 and AA6061 indicated the presence of MgSi₂. Yet, the Mg₂Al₃ may precipitate in the grain boundaries or within the grain of AA5083.

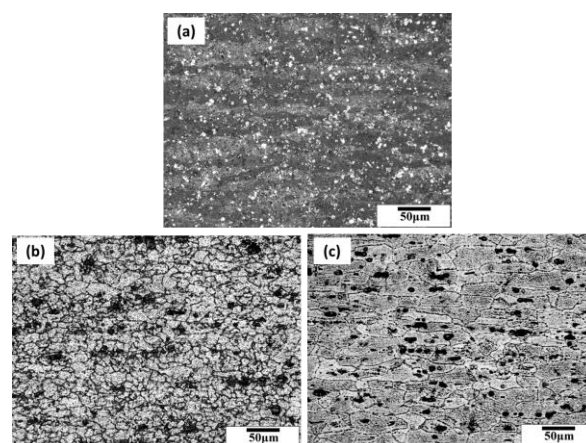


Figure 2 Microstructure of base metal a) AA1100 b) AA5083 c) AA6061

3.2 Visual Assessment

Figure 3 shows the visual assessment on the surface of welding. The ripples on the welding surfaces appeared due to the rotation of the pin shoulder during the stirring process. Furthermore, the ripples followed the rotation direction of the pin shoulder. At the end of the joints, the pin exited through an exit hole. An exit hole is the negative shape of the pin tool that is left after the welding process has stopped. From the image explained that the welded surfaces are clear from the holes and cracks. Figure 3(a) shows the smooth surface with the ribbon flash at the both side of welding path, whereas, Figure 3(b) indicates the smoother welding surface without any ribbon flash. In fact, the geometry of pin used in this work has contributed to the good joining. It has been supported by the previous researcher that dissimilar joints using FSW shows the best welding condition when using the cylindrical threaded pin [13]. The welding burr occurred on the welding surface due to sticking materials during the stirring process of FSW [14]. Whereas, the ribbon welding flash appeared at both sides of AW61 was due to excessive penetration

of the pin tool into the materials which led to the splash of materials out of pin shoulder [15].

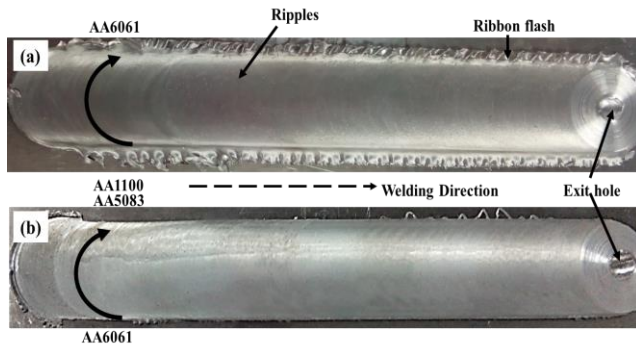


Figure 3 A top view of FSW welds a) AW61 b) AW65

Furthermore, the suitable pin length and pin shoulder as well as tilt angle should be appropriate with the thickness of base metal in order to form a sound welding [16]. The presence of welding surface can be related to the heat input induced from the rotation and traveling speed of pin tool [14]. The traveling and rotation speed determine the heat input during the joining process, as well as, the mechanical properties of materials.

In this work, the strong materials such as AA5083 and AA6061 are located at the advancing side of AW-65 and AW-61, respectively. The locations of these materials are encouraging the effectiveness of welding. It is worth mentioning that the strong force from advancing side is encourage the high strength materials to experience high plastic deformation and led to mix with the metal at the retreating side. Further, less welding flash appeared at AW65 compared to AW61 due to high heat input occurred in the joining. Hence, smoother surface contributed to the quality of welding joint by decrease the shear stress in area under the pin shoulder [17].

3.3 Macrostructures of Welded Cross Section

The macrostructure of cross section on the welded region of two samples are shown in Figure 4. The welding cross section describes that the both joints are free from internal defect and pores. Figure 4(a) and 4(b) displayed the macrostructure of welded cross section of AW65 and AW61, respectively. This indicates that the welding parameters and the simple threaded pin used in this work are reasonable to form a defect-free weld region. Moreover, the rotation speed 1000rpm is suitable for joining dissimilar materials since it has been provide sufficient heat input [13].

The colour contrast observed in the image indicates the mixing of two different materials in the FSW region. AA6061 appears darker compared to AA1100 in AW61, whereas in AW65, AA6061 is lighter in colour compared to AA5083. The colour contrast attributed from the chemical etching, in which the materials flow in the nugget zone shows different

pattern due to the stirring process. As shown in Figure 4(a), the material from advancing side AA5083 is on the top of nugget zone. The AA6061 is more sensitive to flow and softening at high temperature, and easily forms plastic deformation, while AA5083 is more steady in softening at high temperature, led to unmixed materials in the nugget zone [19]. Meanwhile, in the Figure 4(b) indicated the lobe shape of AA6061 in the nugget zone, but still no intermixing of AA1100 and AA6061, however the materials from advancing side still on the top of nugget zone. Therefore, it is suggested that the flow ability of different materials has influence to the mixing pattern in the joining region.

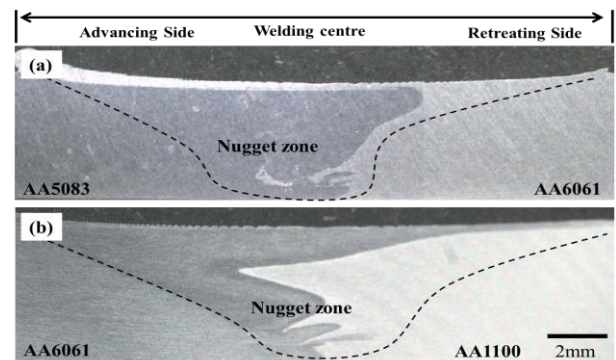


Figure 4 Macrostructure on the cross section of dissimilar welded joint a) AW65 b) AW61

Meanwhile, joining of AW61 is shows a layer between two materials. The AA1100 experienced rapid grain growth that led to softening during the stirring process and hard to flow into AA6061 [20]. Hence, the both materials are mixing but do not well combine by each other. In this case, the materials from advancing side located on the top of welded joints because of dissimilar mechanical behaviour of materials flow during FSW, even though the same welding parameters and tool pin were used during the FSW process.

3.4 Microstructures of Welded Cross Section

In particular, different type of materials entails dissimilar materials flow and it will attribute to the variety of patterns in the stirred zone. As shown in Figure 5, the pattern of microstructure at the nugget zone was observed using the weck reagent. It has been discovered that the nugget zone in AW65 appeared to be distorted and had a wavy pattern in due to two different base metals that had been mixed up during the FSW process. Whereas, the lobes pattern in the nugget zone of AW61 revealed the motion of pin that enforced the materials under the pin shoulder to form any pattern. The mixing pattern depends on the different flows, but not because of chemical mixing [18]. The pattern formed in nugget zone was due to the motion of plasticized materials under the rotating shoulder.

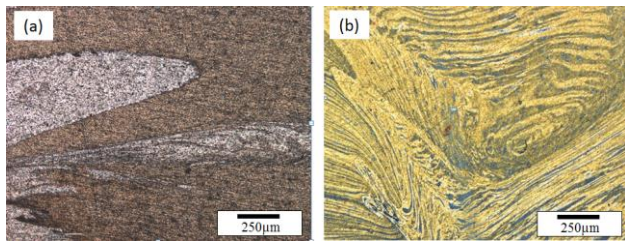


Figure 5 Microstructural pattern at the NZ a) AW61 b) AW65

Figure 6 shows the grain at various zones in welded regions including HAZ, TMAZ and NZ for advancing and retreating side of both joints. Three different zones can be distinguished based on the grain structure at advancing and retreating side. It is appeared the grains were heavily deformed in the TMAZ region towards the nugget zone. The deformation of TMAZ structure is owing to high stress and large deformation occurring due to the mechanical force of the rotating pin, but not up to the recrystallization structure [21]. The TMAZ grains at the advancing side are noticeable as abrupt microstructure compared to retreating side. The significant abruptness at advancing side is common in FSW process, as the same condition was found at the TMAZ grains of advancing side of AW61 [22]. Grain size at the nugget zone consists of more equiaxed at the both welded joints which are 9µm and 15µm of AW65 and AW61 respectively. The equiaxed and fine grained normally obtained at nugget zone in which affected from dynamic recrystallization during FSW process.

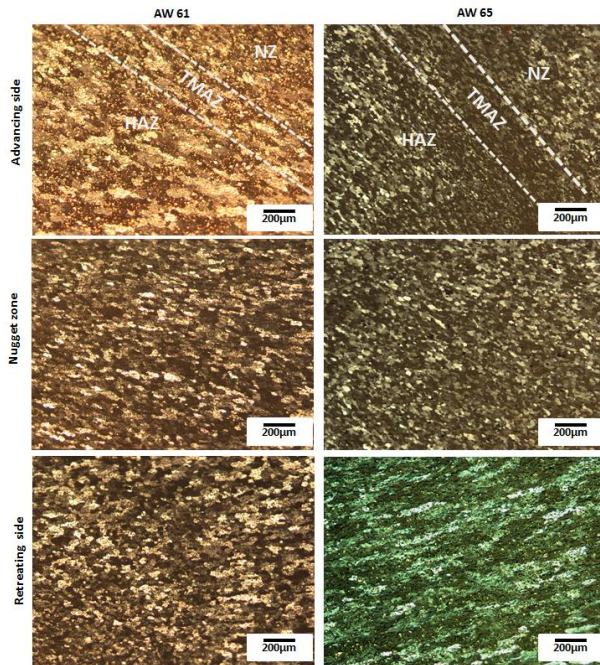


Figure 6 Microstructure shows the different grains size at the Heat Affected Zone, Thermal Mechanical Affected Zone and Nugget Zone at welding joints

As seen in Figure 6, the grain at TMAZ is finer compared to the grains at HAZ, since the TMAZ experienced heat and mechanically affected from the stirring process of welding. The grain size of TMAZ in AW65 and AW61 at the advancing side is 8µm and 9µm, respectively, while the grain size at HAZ of AW65 and AW61 are 12µm and 18µm for the advancing side, respectively. Therefore, the grain structure of materials will exhibit varieties size in each zone.

3.5 Hardness Profile on the Welded Cross Section

FSW of dissimilar materials joint gives significant apparent impact in the mechanical properties of welded regions, especially on the hardness test. Figure 7 shows a micro-hardness profile taken at the middle of thickness along the welded cross section as well as included the base metal. The welding zone shows that the limit of influenced area under the tool shoulder and the outer sides is the hardness of base metals. From the hardness profile, it shows that the hardness of AW65 was constant at about 90HV at the base metal AA5083, but slightly decreased to 80HV when entering the welded zone. In this joint, the hardness continuously decreased from 80HV to 45HV starting from the nugget zone towards AA6061. The hardness declined at the nugget zone could be due to the lack of mixing between AA5083 and AA6061. The lowest hardness value was found at TMAZ of the retreating side with values close to 42HV. On the other hand, the AA6061 base metal shows constant hardness values. The same profile hardness has obtained by other researcher [23].

From the hardness profile, it can be seen that the hardness decreased from the advancing side to retreating side, owing to the low mechanical properties of AA6061 compared to AA5083. However, different values of hardness in the advancing and retreating side gave no effect on the quality of the welding. It is because the tensile fracture occurred at AA6061 base metal outside the welding area, that means the welded joints is stronger than base metal.

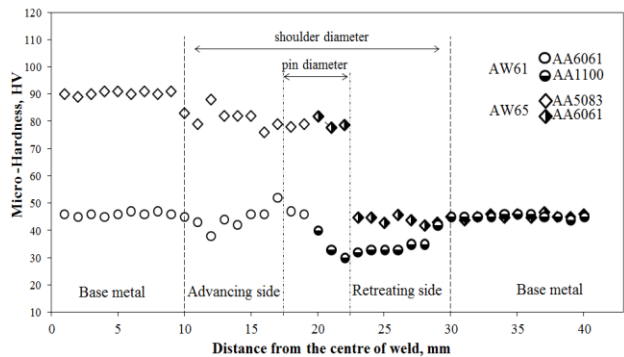


Figure 7 Micro-hardness profile of cross section on welded cross section of AW61 and AW65

On the other hand, the joint of AW61 revealed a constant hardness at base metal AA6061, but reduced from 42HV to 38HV at TMAZ's advancing side when entering the welded region. The hardness dropped at AA6061 because of the effect from the stirring of pin during the FSW process, since AA6061 is a heat-treatable aluminium alloy and effected from temperature distribution during the welding process. From the profile, it can be seen that the hardness decreased from 46HV to 30HV from the nugget zone to the retreating side and subsequently increased up to the base metal AA1100. Usually for the heat-treatable aluminium alloys the "W" shape appearance for hardness will occurred, whereas the HAZ recorded the lowest values due to heat employed during FSW [13].

3.6 Tensile Strength of Joints

Above all, the location of stronger materials at the advancing side will improve joint efficiency. So that the AA5083 and AA6061 should be located at the advancing side in order to produce high strength of joints. The location of materials in advancing and retreating side can determine to form sound welding since the distribution of temperature gives the different thermal behaviour of materials flow [24].

The tensile strength and elongation of base metal and the welded joints has displayed in Figure 8. As can be seen from the graph, the tensile of base metal AA5083 is noticeably higher compared to the other base metals, whereas base metal AA6061 and AA1100 have an almost similar elongation. The tensile strength of AW65 is slightly higher than AW61, with almost similar elongation. The tensile strength and elongation of AW65 is 113MPa and 15%, while, AW61 is 93MPa and 13%, respectively. The joint efficiency of the welded joint can be calculated based on the ultimate tensile strength of welded joint and base metal. Therefore, the joint efficiency of AW61 and AW65 is 80% and 97% when comparing to base metal AA6061.

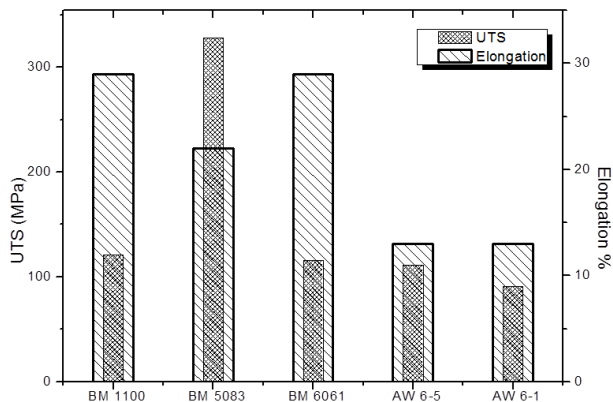


Figure 8 Tensile strength and elongation of base metal and welded joints

In order to comprehend the nature of fractures, the samples were examined using SEM. The morphologies of the fracture surface are shown in Figure 9. Figure 9(a) shows that AW61 was fractured in the welded area at the retreating side of AA1100, while the AW65 was broken outside of the welded area at the base metal AA6061.

Normally, when the superplastic deformation reaches a maximum limit, it will create a nucleation of cavities. The cavities have coalesced to form dimples that grow into the void, causing the fractures [25]. Figure 9 (a) and (c) shows the necking occurred before the samples failed. The necking behaviour indicated high elongation of welded joints. Therefore, from the Figure 8, it shows that the elongation for AW61 and AW65 joints have almost similar value. Moreover, varies size of dimples on the welded surface proves that the samples were failed in ductile behaviour. However, there a lot of big and shallow dimples on the AW61 surface. While the small and depth dimples are obtained on the AW65 surface. Small and depth dimples are related to the high strength of joints, whereas the fractures surface consist of shallow dimples has lower strength.

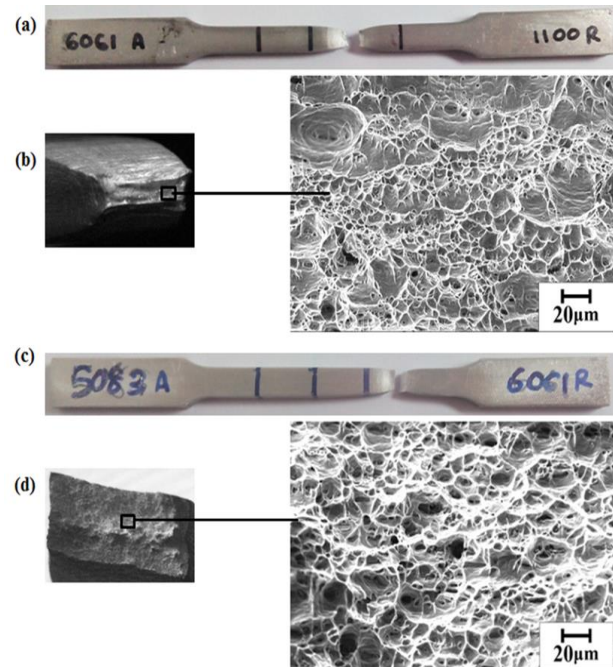


Figure 9 Fractography images of welded sample a) AW61 b) Surface of AW61 c) AW65 d) Surface of AW65

4.0 CONCLUSION

The dissimilar joints of AW65 and AW61 aluminum alloys had been successfully welded and the results are as follows. Both dissimilar welded joints have a smooth welding surface, but the welding flash was obtained at AW61 instead of AW65. The differing mechanical properties of the materials resulted in different pattern flows during the FSW process, which means that both joints showed no intermixing

between the materials at the nugget zone, but the materials at the advancing side was located at the top of the joint. The joint efficiency of the welded joint were outstanding when compared to the base metal AA6061, reported to be 97% and 80% for AW65 and AW61, respectively. This confirmed the excellent weldability of dissimilar joint aluminum alloys using the FSW method at specific welding parameters.

Acknowledgement

The authors would like to express their gratitude to the Ministry of Higher Education, Malaysia (MOHE) through Universiti Kebangsaan Malaysia (UKM) for financial grants, project no, FRGS/1/2013/TK01/UKM/02/4. We are also indebted to Sharif University Technology, Tehran, Iran for assistance in FSW.

References

- [1] Threadgill, P. J., Leonard, P. L., Shercliff, A. J., Withers, H. R. 2009. Friction Stir Welding of Aluminium Alloys. *International Materials Review*. 54: 43-93.
DOI: <http://dx.doi.org/10.1179/174328009X411136>.
- [2] Mishra, R. S., Mahoney, W. 2007. Friction Stir Welding and Processing. *Asm International*. 3-55.
DOI: 10.1361/fswp2007p001.
- [3] Mishra, R. S., Ma, Z. Y. 2005. Friction Stir Welding and Processing. *Materials Science and Engineering R: Report*. 50: 1-78.
DOI: <https://doi.org/10.1016/j.mser.2005.07.001>.
- [4] Rodrigues, D. M., Leitão, C., Louro, R., Gouveia, H., Loureiro, A. 2010. High Speed Friction Stir Welding of Aluminium Alloy. *Science Technology Welding Joining*. 15: 676-81.
DOI: 10.1179/136217110X12785889550181.
- [5] Liu, K., Fuji, H., Maeda, H., Nogi, M. 2006. Friction Stir Weldabilities of AA1050-H24 and AA6061-T6 Aluminium Alloys. *Journal Material Science Technology*. 21: 415-18.
DOI: 10.3321/j.issn:1005-0302.2005.03.027.
- [6] Derazkola, H. A., Elyasi, M., Hossienzadeh, M. 2014. Feasibility Study on Aluminium Alloys and A441 Steel Joints by Friction Stir Welding. *Int. Journal Advances Design Manufacturing Technology*. 7: 99-109.
URL: http://admt.sinaweb.net/article_534909.html.
- [7] Ilangovan, M., Boopathy, S. R., Balasubramanian, V. 2015. Microstructure and Tensile Properties of Friction Stir Welded Dissimilar AA6061 and AA5086 Aluminium Alloy Joints. *Trans. Nonferrous Met. Soc. Chin*. 25: 1080-90.
DOI: <https://doi.org/10.1016/j.dt.2015.01.004>.
- [8] Palanivel R, Koshy Mathews P, Dinaharan I, Murugan N. 2014. Mechanical and Metallurgical Properties of Dissimilar Friction Stir Welded AA5083-H111 and AA6351-T6 Aluminium Alloys. *Trans. Nonferrous Met. Soc. Chin*. 24: 58-65.
DOI: [https://doi.org/10.1016/S1003-6326\(14\)63028-4](https://doi.org/10.1016/S1003-6326(14)63028-4).
- [9] Amini, P., Asadi, A. 2014. Friction stir Welding Application in Industry. *Advances in Friction-stir Welding and Processing*. Elsevier. 671-722.
DOI: 10.1533/9780857094551.671
- [10] Kissell, J. R., Pantelakis, S. G., Haidemenopoulos, G. N. 2004. Aluminum and Aluminum Alloy. *Handbook of Advanced Materials*: Wiley. 326-77
DOI: 10.1002/0471465186.ch9.
- [11] Gan W, Okamoto K, Hirano S, Chung K. 2008. Properties of Friction Stir Welded Aluminium Alloys 6111 and 5083. *Journal of Engineering Materials and Technology*. 130: 1-15.
DOI: 10.1115/1.2931143
- [12] Uematsu Y, Tokaji K, Shibata H, Tozaki Y, Ohmune T. 2009. Fatigue Behavior of Friction Stir Weld without neither Welding Flash nor Flaw in Several Aluminium Alloys. *Int. Journal of Fatigue*. 31: 1443-53.
DOI: <https://doi.org/10.1016/j.ijfatigue.2009.06.015>
- [13] Jayaraman M, Balasubramanian V. 2013. Effect of Process on Tensile Strength of Friction Stir Welded Cast A356 Aluminium Alloys Joints. *Trans. Nonferrous Met. Soc. Chin*. 23: 605-15.
DOI: 10.1016/S1003-6326(13)62506-6.
- [14] Sathari N. A., Razali A, Ishak M, Shah L. 2015. Mechanical Properties and Temperature Distribution of Thin Friction Stir Welded Sheets of AA5083. *Int. J. of Auto Mech. Eng*. 2713-21.
DOI: 10.5923/j.mechanics.20120201.01.
- [15] Arbegast W. J. 2008. A flow-Partitioned Deformation Zone Model for Defect Formation during Friction Stir Welding. *Scr. Mater*. 58: 372-76.
DOI: 10.1016/j.scriptamat.2007.10.031.
- [16] Serio L, Palumbo D, De Filippis L, Galletti U, Ludovico A. 2016. Effect of Friction Stir Process Parameters on the Mechanical and Thermal Behavior of 5754-H111 Aluminium Plates. *Materials (Basel)*. 9: 2-19.
DOI: 10.3390/ma9030122
- [17] Dawood H. I., Mohamed S. K., Rahmat A, Uday M. B. 2015. The Influence of the Surface Roughness on the Microstructures and Mechanical Properties of 6061 Aluminium Alloy Using Friction Stir Welding. *Trans. Nonferrous Met Soc. Chin*. 25: 2856-65.
DOI: 10.1016/j.surfcoat.2015.02.045.
- [18] Amancio-Filho S. T., Sheikhi S, Dos Santos J. F., Bolfarini C. 2008. Preliminary Study on the Microstructure and Mechanical Properties of Dissimilar Friction Stir Welding in Aircraft Aluminum Alloys 2024-T351 and 6056-T4. *J. Mater. Process. Technol*. 206: 132-42.
DOI: 10.1016/j.jmatprotec.2007.12.008.
- [19] Son H. J., Park S. K., Hong S. T., Park J. H, Park K. Y, Kwon Y. J. 2010. Effect of Materials Locations on Properties of Friction Stir Welding Joints of Dissimilar Aluminium Alloys. *Sci. Technol. Weld. Joining*. 15: 331-36.
DOI: <http://dx.doi.org/10.1179/136217110X12714217309696>
- [20] Sun Y. F., Fujii H, Tsuji M. 2013. Microstructure and Mechanical Properties of Spot Friction Stir Welded Ultrafine Grained 1050 Al and Conventional Grained 6061-T6 Al Alloys. *Mater. Sci. Eng*. 585: 17-24.
DOI: 10.1016/j.msea.2013.07.030.
- [21] Rajamanickam N, Balusamy V, Madhusudhanna Reddy G, Natarajan K .2009. Effect of Parameters on Thermal History and Mechanical Properties of Friction Stir Welds. *Mater. Des*. 30: 2726-31.
DOI: 10.1016/j.matdes.2008.09.035.
- [22] Peel M, Steuwer A, Preuss M, Withers P. J. 2003. Microstructure, Mechanical Properties and Residual Stresses as a Function of Welding Speed in Aluminium AA5083 Friction Stir Welds. *Acta Mater*. 51: 4791-801.
DOI: [https://doi.org/10.1016/S1359-6454\(03\)00319-7](https://doi.org/10.1016/S1359-6454(03)00319-7).
- [23] Gungor B, Kaluc E, Taban E, Sik A. 2014. Mechanical, Fatigue and Microstructural Properties of Friction Stir Welded 5083-H111 and 6082-T651 Aluminium Alloys. *Mater. Des*. 56: 84-90.
DOI: <https://doi.org/10.1016/j.matdes.2013.10.090>.
- [24] Gosh M, Kumar K, Kailas S. V, Ray A.K. 2010. Optimization of Friction Stir Welding for Dissimilar Aluminium Alloys. *Mater. Des*. 31:3033-37.
DOI: 10.1016/j.matdes.2010.01.028.
- [25] Sun P. H., Wu H. Y., Lee W. S., Shis S. H., Perng J. Y., Lee S. 2009. Cavitation Behavior in Superplastic 5083 Al Alloy During Multiaxial Gas Blow Forming with Lubrication. *Int. J. Mach Tools Manuf*. 49: 13-19.
DOI: 10.1016/j.ijmactools.2008.08.003.